

# Power of inhibition activity screening and 3D molecular modeling approaches in HDAC 8 inhibitor design

Gamze BORA TATAR<sup>1</sup>, Tenzile Deniz TOKLUMAN<sup>1</sup>, Kemal YELEKÇİ<sup>2,\*</sup>,  
Hayat YURTER<sup>1,\*</sup>

<sup>1</sup>*Department of Medical Biology, Faculty of Medicine, Hacettepe University,  
06100, Sıhhiye, Ankara-TURKEY  
e-mail: herdem@hacettepe.edu.tr*

<sup>2</sup>*Computational Biology and Bioinformatics, Faculty of Arts and Science, Kadir Has University,  
34083, Cibali, İstanbul-TURKEY  
e-mail: yelekci@khas.edu.tr*

Received: 12.07.2011

In-vitro inhibition activity screening and in-silico 3D molecular modeling approaches are important tools for design and development of specific histone deacetylase (HDAC) inhibitors. The objective of this study was to investigate the consistency between these 2 approaches. The HDAC 8 inhibition activities of 8 randomly selected different carboxylic acid derivatives were screened and in-vitro experimental results were compared with in-silico molecular modeling calculations. This study demonstrated that there is no sole gold standard technique for inhibitor design, and it was concluded that a combination of molecular modeling and activity screening assays will ensure more comprehensive and dependable results.

**Key Words:** Carboxylic acids, HDAC 8 inhibitor, activity screening, 3D molecular modeling

## Introduction

Histone deacetylases (HDAC) are a group of enzymes that play an important role in transcription regulation via influencing chromatin packaging status. HDACs remove acetyl groups from histone tails, leading to tighter wrapping of DNA around the histone core. In this way, deacetylation blocks the accessibility of transcription factors to genes and is generally associated with repression of transcription and gene expression.<sup>1</sup> Human HDACs consist of 18 isoforms (HDAC 1-11 and SIRT 1-7). Structures, enzymatic functions, subcellular localizations, and

---

\*Corresponding author

expression patterns of isoforms are different and therefore HDACs have been associated with diverse cellular functions, such as cell differentiation, apoptosis, and cytoskeletal modifications.<sup>2</sup> Increasing evidence shows that disruption of these HDAC related functions is involved in various medical conditions such as cancer, inflammation, and neurodegenerative diseases; therefore inhibiting HDACs is a promising strategy for possible treatment of such conditions.<sup>1-5</sup> Although pan-HDAC inhibitors have been used in clinical trials of various diseases, low efficacy and possible side effects limit their use; hence isoform specific inhibitors have begun to draw more attention.<sup>6-8</sup>

HDAC inhibitors are a structurally diverse group classified as hydroximates, cyclic tetrapeptides, benzamides, electrophilic ketones, and carboxylic acids. All classes contain a common chemical structure consisting of 3 components: a metal-binding functional group, a hydrocarbon linker, and a capping group<sup>9</sup> (Figure 1).

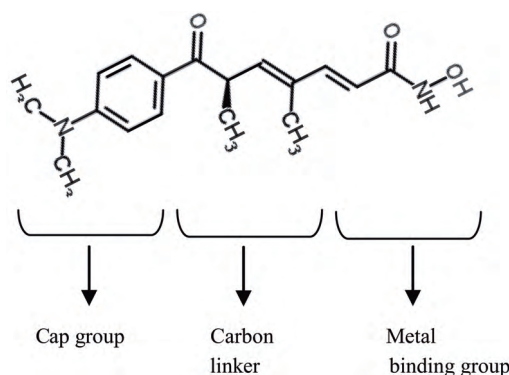


**Figure 1.** Common chemical structure of HDAC inhibitors.

Three components of the common structure can be modified to design and eventually develop more potent and isoform specific inhibitors. In the inhibitor design process, activities of compounds need to be assessed via both in-vitro and in-silico approaches. In the current study, we investigated the consistency between in-vitro screening and in-silico 3D molecular modeling approaches by utilizing HDAC 8 enzyme, which was the first crystallized and the most studied human HDAC isoform.<sup>10-12</sup>

## Materials and methods

### In-vitro HDAC 8 inhibition activity screening

Eight randomly selected carboxylic acid group of HDAC inhibitors (valproic acid, sodium butyrate, cinnamic acid, caffeic acid, chlorogenic acid, rosmarinic acid, curcumin, and quercetin) that have different cap, linker, and metal binding groups were included in the study.<sup>13</sup> HDAC 8 inhibition activities of these compounds were analyzed at 500  $\mu$ M concentration on HeLa nuclear extract via an in-vitro fluorometric assay based on Fluor de Lys®-HDAC 8 (Biomol) substrate, which comprises an acetylated lysine side chain. Deacetylation sensitizes the substrate and produces a fluorophore that was measured with a fluorescence plate reader (350-440 nm). Treated samples were normalized according to non-treated controls, which were set at 100%. A decrease in the fluorescence signal indicates the inhibition potency of compounds. Trichostatin A (TSA) was included in

the study as a control based on its known inhibitory effects on HDAC 8 enzyme and was analyzed at 50  $\mu\text{M}$  concentration.<sup>12,14</sup> Chemical structures of all HDAC inhibitors analyzed in the study are shown in Table 1.

We also utilized an in-vitro fluorometric assay to detect half-maximum HDAC 8 inhibition ( $\text{IC}_{50}$ ) of curcumin with a wide concentration range ( $10^{-11}$ - $10^{-2}$  M). GraphPad Prism software 4.0<sup>15</sup> was used to calculate the dose-response curve via non-linear regression analysis. Concentrations between  $10^{-11}$  and  $10^{-6}$  M that give a plateau were excluded. The highest value of HDAC 8 inhibition was set at 100% and the  $\text{IC}_{50}$  value of curcumin was calculated.

## Crystal structure of HDAC 8

The crystal structure of human HDAC 8 complexed with TSA (coded as 1T64 and its resolution is 1.90 Å) was extracted from the Protein Data Bank (PDB).<sup>16</sup> Its structure was cleaned of all the water molecules and inhibitor as well as all non-interacting ions before being used in docking studies. Only the Zn ion was retained in the active site since it behaves as a cofactor of the enzyme. Using a fast Dreiding-like force-field the protein's geometry was first optimized and then submitted to the "Clean Geometry" toolkit of Discovery Studio<sup>17</sup> (Accelrys 3.00, Inc.) for a more complete check. Missing hydrogen atoms were added based on the protonation state of the titratable residues at pH 7.4. Ionic strength was set to 0.145 and dielectric constant to 10. All the inhibitor molecules were drawn and minimized by the Accelrys' ligand preparation protocol.

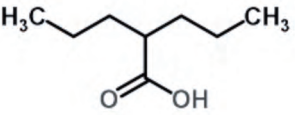
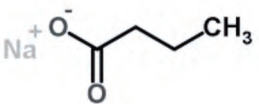
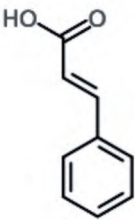
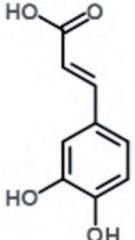
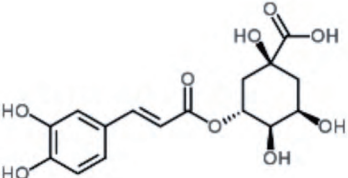
## Docking

AutoDock 4.2<sup>18</sup> uses a semi-empirical force field based on the Amber force field. It uses a molecular mechanics model for enthalpic contributions such as vdW and hydrogen bonding and an empirical model for entropic changes upon binding. Each component is multiplied by empirical weights obtained from the calibration against a set of known binding constants. AutoDock uses the Lamarckian Genetic algorithm for conformational search. For each molecule, 50 independent runs are performed. A total of 300 distinct ligand conformers are initially generated and positioned randomly in the binding pocket. They had randomly assigned torsion angles to rotatable bonds and a randomly assigned overall rotation. A maximum of 100 million energy evaluations are allowed for each docking. A pre-calculated 3-dimensional energy grid of equally spaced discrete points is generated prior to docking, for a rapid energy evaluation, using the program AutoGrid 4.2.<sup>19</sup> The grid box with dimensions of 60 Å  $\times$  60 Å  $\times$  60 Å is centered in the vicinity of the Zn ion and covers the entire binding site and its neighboring residues. The distance between 2 grid points is set to 0.375 Å.

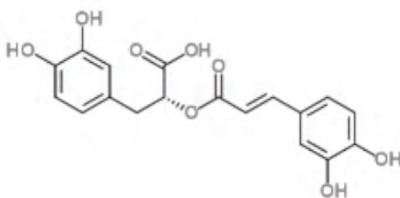
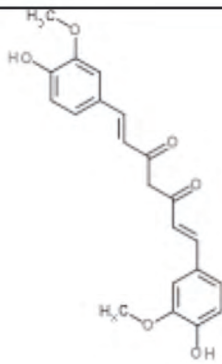
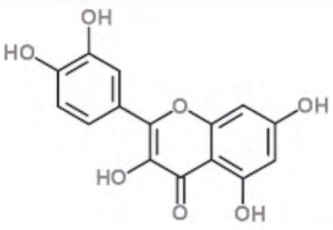
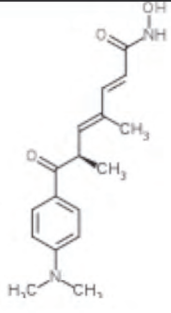
## Results and discussion

HDAC 8 inhibition activities of randomly selected carboxylic acids were analyzed via both inhibition activity screening and molecular modeling approaches. According to our results, these approaches showed modest correlation. In-vitro HDAC 8 inhibition activities and in-silico molecular modeling calculations are given in Table 2; inhibition potencies of the compounds are summarized in Figure 2.

**Table 1.** Chemical structures of HDAC inhibitors.

	Compound Structure	Compound Name
Carboxylic acids		Valproic acid
		Sodium butyrate
Carboxylic acids with cap group modifications		Cinnamic acid
		Caffeic acid
Carboxylic acids with cap and metal binding group modifications		Chlorogenic acid

**Table 1.** Continued.

Carboxylic acids with cap, linker and metal binding group modifications		Rosmarinic acid
		Curcumin
		Quercetin
Hydroximate		TSA

The pose, interaction with the active site chain residues, and the binding energy of TSA agreed with the reported data (Figure 3). According to the results in Table 2, HDAC 8 experimental inhibition activity of the first 4 compounds (curcumin, quercetin, rosmarinic acid, and chlorogenic acid) agreed very well with the computational inhibition values. However, the last 4 compounds showed higher computational values in

**Table 2.** In-vitro HDAC 8 inhibition activities and in-silico 3D molecular modelling calculations (free energy of bindings and inhibition constants).

Compound name	HDAC 8 inhibition activity (%)	Free energy of binding ( $\Delta G$ kcal/mol)	Inhibition constant
Curcumin	88	-7.65	2.45 $\mu M$
Quercetin	82	-7.15	5.72 $\mu M$
Rosmarinic acid	68	-6.47	17.99 $\mu M$
Chlorogenic acid	65	-6.12	32.39 $\mu M$
TSA*	63	-7.50	3.30 $\mu M$
Sodium butyrate	42	-9.36	137.13 nM
Caffeic acid	35	-9.91	54.02 nM
Valproic acid	23	-11.45	4.05 nM
Cinnamic acid	6	-10.64	15.93 nM

\*TSA was analyzed at 50  $\mu M$  concentration

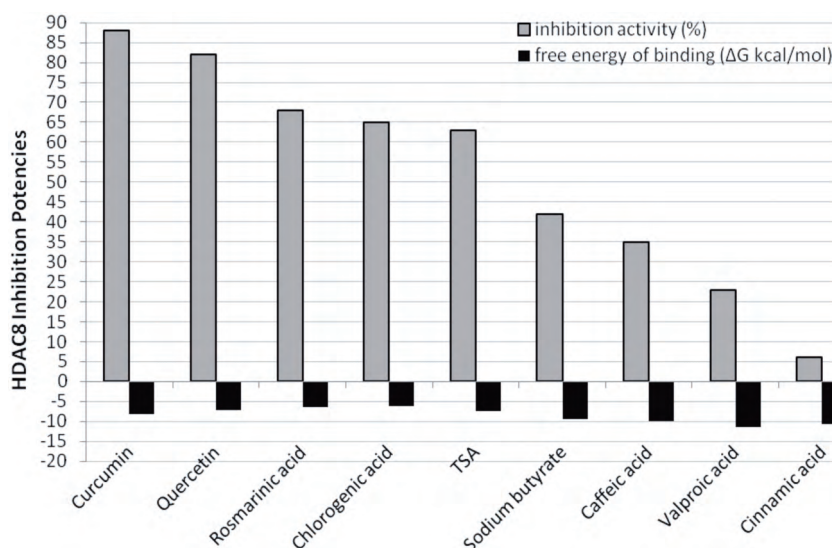


**Figure 2.** HDAC 8 inhibition potencies of compounds according to in-vitro (gray bars) and in-silico (black bars) analyses.

comparison to experimental values. We found that small carboxylic acids and their ionized form (sodium butyrate) get into the active site as deep as possible and make a more efficient interaction with the cofactor zinc ion and the other residues such as Tyr306 (hydrogen bond), His142, and Asp267 in the active site (valproic acid in Figure 4). The polar active site residues have little interactions with hydrophobic side chains. We also found that there is another important relatively hydrophobic binding region aside from the active site comprising Lys33, Ala32, Ile34, Pro35, Phe152, Arg37, Trp141, Cys28, and Tyr111. From Figures 5 (rosmarinic acid),

6 (quercetin), and 7 (curcumin) it is seen that all these compounds bind to this site. Small carboxylic acids such as valproic acid may also bind to this hydrophobic region in addition to the active site showing rather low affinity to HDAC 8 isozyme in this site. The experimental low affinity values of the small carboxylic acids may be speculated based on the fact that they may also experimentally bind to this site.

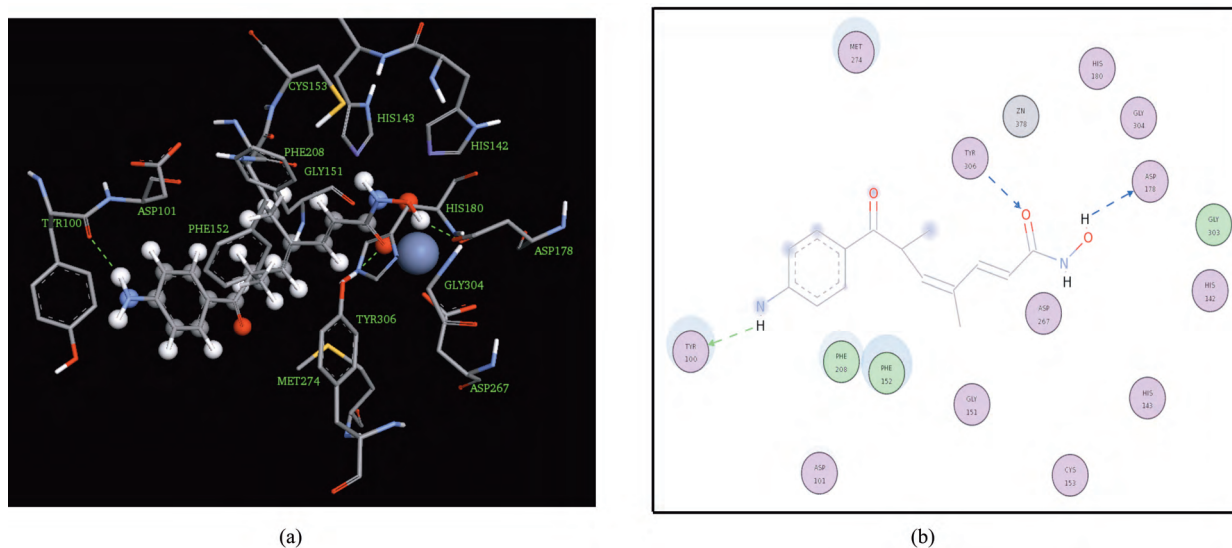


**Figure 3.** Three-dimensional orientation of TSA in the active site of HDAC 8. Amino acid side chains are shown as sticks, inhibitor is shown as ball and stick, and cofactor Zn is depicted as gray ball in all 3D pictures (a). Two-dimensional picture of TSA in the active site of HDAC 8 enzyme. Residues involved in hydrogen bonding or polar interactions are represented by magenta circles, and residues involved in vdW and hydrophobic interactions are shown by green circles in all 2-dimensional figures (b).

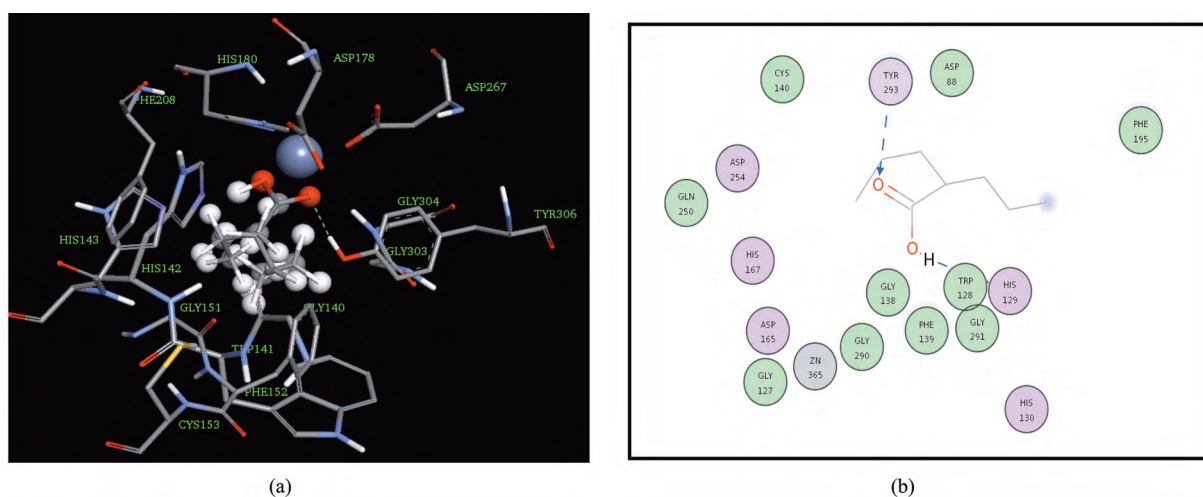


**Figure 4.** Valproic acid is shown in the active site (3D) of HDAC 8 (a). Valproic acid is shown in the active site (2D) of HDAC 8 (b).



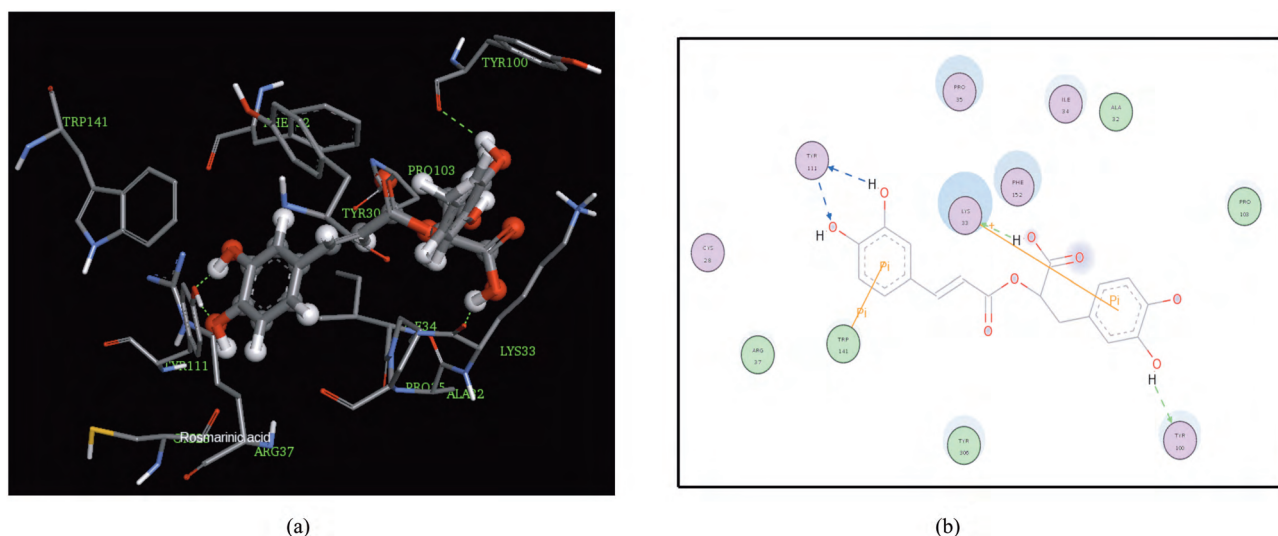


**Figure 5.** Rosmarinic acid is shown in the active site (3D) of HDAC 8 (a). Rosmarinic acid is shown in the active site (2D) of HDAC 8 (b).

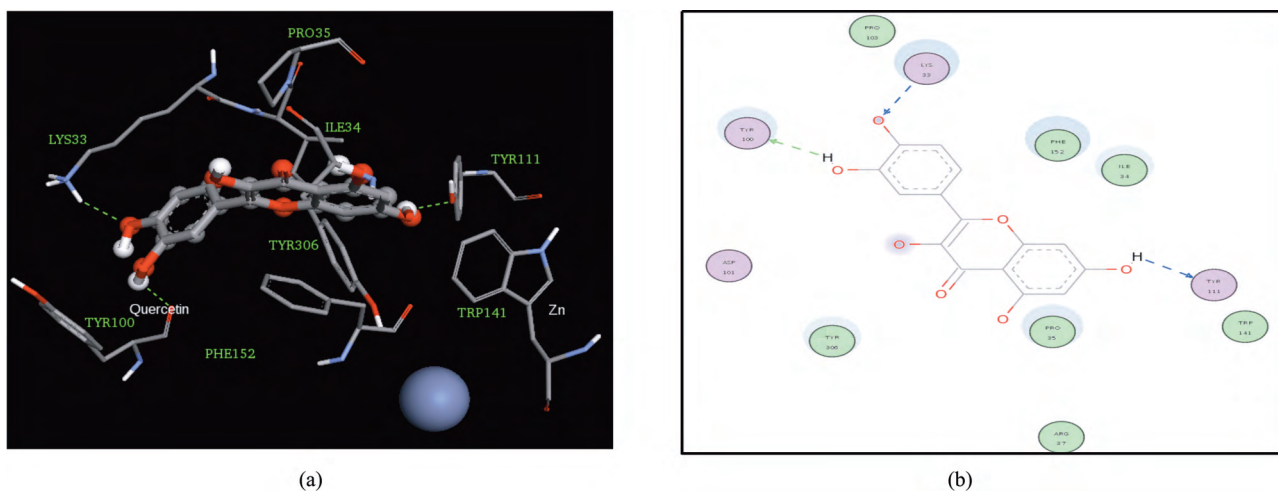


**Figure 6.** Quercetin is shown in the active site (3D) of HDAC 8 (a). Quercetin is shown in the active site (2D) of HDAC 8 (b).

According to the in-vitro experimental results, curcumin had the highest HDAC 8 inhibition activity but it possessed moderate free energy of binding and inhibition constant values among the tested compounds (Table 2, Figure 7). In order to improve the experimental result, half-maximum HDAC 8 inhibition of curcumin was determined. The dose-response curve of curcumin was calculated by non-linear regression analysis and the  $IC_{50}$  value of curcumin was calculated as  $642 \mu\text{M}$  (Figure 8). Comparison of curcumin with PCI-34051, which is a potent HDAC 8 specific inhibitor ( $IC_{50}$ :  $0.01 \mu\text{M}$ ), showed that curcumin had moderate HDAC 8 inhibition activity, which is supported by our computational results.<sup>20</sup>



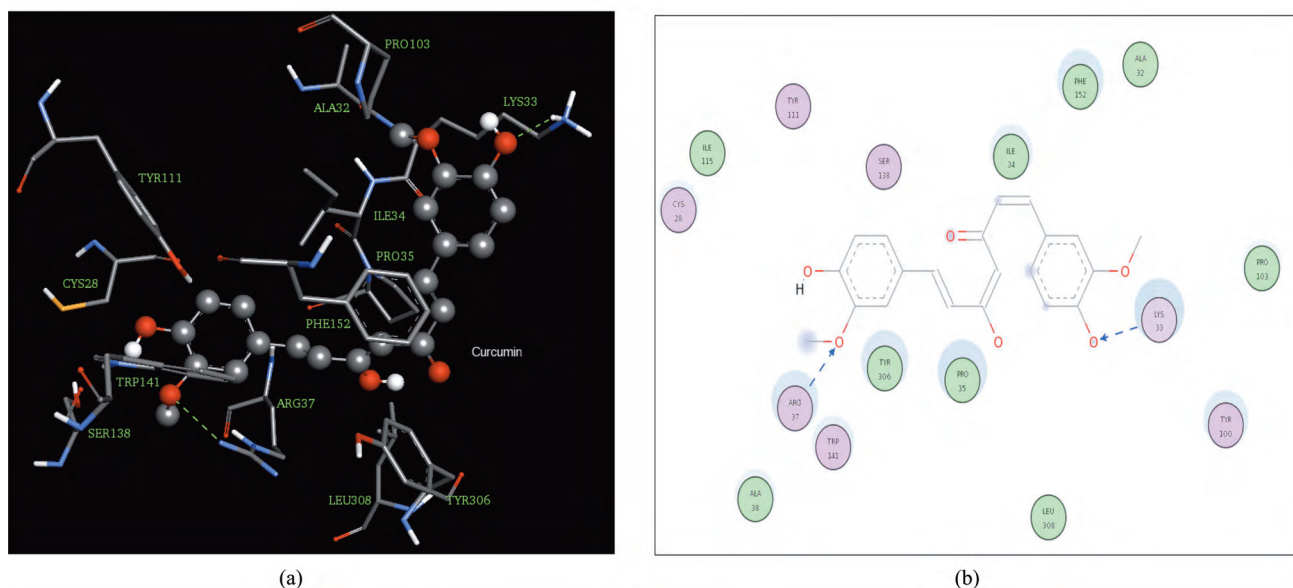


**Figure 7.** Curcumin is shown in the active site (3D) of HDAC 8 enzyme (a). Curcumin is shown in the active site (2D) of HDAC 8 enzyme (b).

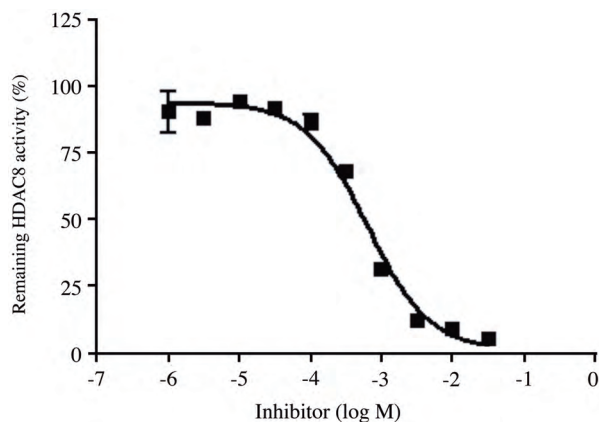


**Figure 8.** Half-maximum HDAC 8 inhibition by curcumin,  $IC_{50}$ : 642  $\mu$ M.

The results of the 2 approaches suggest that both methods should be considered together in designing new inhibitors. Commercially available HDAC inhibition assays are generally based on fluorometric or colorimetric analyses. These assays are useful for quick screening of potential compounds but results should be confirmed via  $IC_{50}$  calculations with a broadened concentration spectrum. Moreover, development of more sensitive tests will help to eliminate confusing results.

The 3D molecular modeling approach has become increasingly important in drug design and development processes.<sup>8,21</sup> The major limiting factor is that only 4 crystal structures of human HDACs (HDAC 2, 4, 7, and 8) are available in protein databanks.<sup>7,16</sup> In this regard, further crystallographic analyses for human HDAC isoforms will accelerate the design of new isoform specific inhibitors. Advanced molecular modeling software

and computational facilities will also help to generate more accurate protein-inhibitor binding modes. Taken together, there is no sole gold standard technique for inhibitor design. Combination of molecular modeling and activity screening assays will help to ensure more comprehensive and dependable results.

## Acknowledgement

We acknowledge Prof. Dr. Sevim Dalkara from Hacettepe University's Faculty of Pharmacy for providing the compounds for this study.

## References

1. Haberland, M.; Montgomery, R. L.; Olson, E. N. *Nat. Rev. Genet.* **2009**, *10*, 32-42.
2. Marsoni, S.; Damia G.; Camboni, G. *Epigenetics* **2008**, *3*, 164-172.
3. Paris, M.; Porcelloni, M.; Binaschi, M.; Fattori, D. *J. Med. Chem.* **2008**, *51*, 1505-1529.
4. Hahnen, E.; Hauke, J.; Tränkle, C.; Eyüpoglu, I. Y.; Wirth, B.; Blümcke, I. *Expert Opin. Investig. Drugs.* **2008**, *17*, 169-184.
5. Sleiman, S. F.; Basso, M.; Mahishi, L.; Kozikowski, A. P.; Donohoe, M. E.; Langley, B.; Ratan, R. R. *Expert Opin. Investig. Drugs.* **2009**, *18*, 573-584.
6. Balasubramanian, S.; Verner, E.; Buggy, J. J. *Cancer Lett.* **2009**, *280*, 211-221.
7. Bieliauskas, A. V.; Pflum, M. K. *Chem. Soc. Rev.* **2008**, *37*, 1402-1413.
8. Zhang, L.; Fang, H.; Xu, W. *Med. Res. Rev.* **2010**, *30*, 585-602.
9. Marks, P. A.; Richon, V. M.; Miller, T.; Kelly, W. K. *Adv. Cancer Res.* **2004**, *91*, 137-168.
10. Vannini, A.; Volpari, C.; Filocamo, G.; Casavola, E. C.; Brunetti, M.; Renzoni, D.; Chakravarty, P.; Paolini, C.; De Francesco, R.; Gallinari, P.; Steinkühler, C.; Di Marco, S. *Proc. Natl. Acad. Sci. U. S. A.* 2004, *101*, 15064-15069.
11. Vannini, A.; Volpari, C.; Gallinari, P.; Jones, P.; Mattu, M.; Carfi, A.; De Francesco, R.; Steinkühler, C.; Di Marco, S. *EMBO Rep.* 2007, *8*, 879-884.
12. Somoza, J. R.; Skene, R. J.; Katz, B. A.; Mol, C.; Ho, J. D.; Jennings, A. J.; Luong, C.; Arvai, A.; Buggy, J. J.; Chi, E.; Tang, J.; Sang, B. C.; Verner, E.; Wynands, R.; Leahy, E. M.; Dougan, D. R.; Snell, G.; Navre, M.; Knuth, M. W.; Swanson, R. V.; McRee, D. E.; Tari, L. W. *Structure* **2004**, *12*, 1325-1334.
13. Bora-Tatar, G.; Dayangaç-Erden, D.; Demir, A. S.; Dalkara, S.; Yelekçi, K.; Erdem-Yurter, H. *Bioorgan Med. Chem.* **2009**, *17*, 5219-5228.
14. He, J.; Liu, H.; Chen, Y. J. *Huazhong Univ. Sci. Technol. Med. Sci.* **2006**, *26*, 531-533.
15. Graphpad Prism Software version 4.0., La Jolla California, U.S.A.
16. <http://www.rcsb.org>. The Protein Data Bank. Berman, H. M.; Westbrook, J.; Feng, Z.; Gilliland, G.; Bhat, T. N.; Weissig, H.; Shindyalov, I. N.; Bourne, P. E. *Nucleic Acids Res.* **2000**, *28*, 235-242.
17. Accelrys Software Inc, Discovery Studio, Release 3.00, San Diego, USA: Accelrys Software Inc., 2007.
18. Morris, G. M., Goodsell, D. S., Halliday, R. S., Huey, R., Hart, W. E., Belew, R. K.; Olson, A. J. *J. Comput. Chem* **1998**, *19*, 1639-1662.
19. Morris G. M.; Huey, R.; Lindstrom, W.; Sanner M. F.; Belew R. K.; Goodsell D. S.; Olson A. J. *J Comput Chem.* **2009** *30*, 2785-2791.
20. Balasubramanian, S.; Ramos, J.; Luo, W.; Sirisawad, M.; Verner, E.; Buggy, J. J. *Leukemia* **2008**, *22*, 1026-34.
21. Wang, D. *Curr. Top. Med. Chem.* **2009**, *9*, 241-256.